Supplement of Atmos. Chem. Phys., 26, 7311–7324, 2026
https://doi.org/10.5194/acp-26-7311-2026-supplement

Atmospheric Chemistry and Physics
Open Access
EGU

Supplement of

Highly viscous phase behavior of organic-rich urban $PM_{2.5}$

Atta Ullah et al.

Correspondence to: Mijung Song (mijung.song@jbnu.ac.kr)

S1. Extraction and droplet generation from $PM_{2.5}$ filters

The quartz filters containing $PM_{2.5}$ were cut into small pieces and extracted using a 1:1 (v/v) methanol-water solution, where methanol was high-performance liquid chromatography grade (Sigma-Aldrich), and water had a resistivity of 18.2 MΩ·cm (Millipore, USA). This methanol–water mixture is commonly used for extracting $PM_{2.5}$ components from filters for chemical analysis because it efficiently recovers both hydrophilic inorganic constituents and hydrophobic organic species across a wide range of polarities (Choi et al., 2017; An et al., 2019; Kim et al., 2025). After extraction, the solution was sonicated for 1 hr at ~290 K and then filtered through a poly(ether sulfone) membrane with a 0.05 μm pore size. Micrometer-scale droplets were subsequently generated from the filtered extract using a nebulizer (MEINHARD, PerkinElmer, USA) and deposited onto a hydrophobic substrate (Hampton Research, Canada) (Song et al., 2025). This method primarily captures the water and methanol-soluble fraction of $PM_{2.5}$, as insoluble components are removed during filtration.

S2. Chemical compositions of $PM_{2.5}$

The hourly mass concentration of $PM_{2.5}$ was measured by a β-ray continuous ambient particle sensor (Thermo Scientific Inc., model 5014i, USA). The mass concentrations of inorganic ions, such as NO_3^-, SO_4^{2-}, NH_4^+, Cl^-, Na^+, Ca^{2+}, K^+, and Mg^{2+} were determined by ion chromatography (AQUION, Thermo Scientific, Massachusetts, USA) following procedures described in a previous study (Won et al., 2024). The mass concentrations of ammonium nitrate (AN) and ammonium sulfate (AS) were calculated from the measured nitrate and sulfate concentrations using Eqs. (S1) and (S2), respectively (Lan et al., 2018; Xue et al., 2023).

$$AN = NO_3^- \times 1.290 \quad \text{(S1)}$$

$$AS = SO_4^{2-} \times 1.375 \quad \text{(S2)}$$

The mass concentration of organic matter (OM) was determined by subtracting the concentrations of inorganic compounds from the total $PM_{2.5}$. Meteorological parameters, including temperature and RH, were measured by the National Institute of Environmental Research in Seoul and an automated meteorological station (Met One Instruments, Inc., USA) in Beijing (Kim et al., 2022; Qiu et al., 2023). All meteorological data were averaged according to the filter sample intervals (from 10:00 to 09:00 local time the subsequent day). The O:C ratio of water-soluble organic compounds (WSOC) in the $PM_{2.5}$ filter-collected sample was measured by employing the Fourier-transform ion cyclotron resonance mass spectrometer (FT-ICR MS) as detailed in previous studies (Choi et al., 2017; Song et al., 2022).

S3. Conditioning time of $PM_{2.5}$ droplets under controlled RH conditions

In the poke-and-flow experiment, $PM_{2.5}$ droplets with a diameter of ~40 μm were deposited on a hydrophobic substrate and allowed to equilibrate under the specified RH of the carrier gas. To verify whether the droplets approached near-equilibrium with the target RH, we applied a previously established method that incorporates measured viscosity values and the corresponding water diffusion coefficient (Evoy et al., 2021; Maclean et al., 2021; Smith et al., 2021;

Kiland et al., 2023). This approach compares the experimental conditioning time with the characteristic mixing time of water within organic aerosol (OA), $\tau_{mix,\ H_2O}$, calculated as follows:

$$\tau_{mix,H2O} = \frac{{d_p}^2}{4\pi^2 D_{H2O}(T, RH)} \quad \text{(S3)}$$

Here, d_p represents the particle diameter. $D_{H_2O}(T,\ RH)$ is the RH- and temperature-dependent diffusion coefficient of water in OA. The value of $D_{H_2O}\ (T, RH)$ was calculated using the fractional Stokes–Einstein equation, which considers the relationship between viscosity and diffusion when the diffusing species are comparable in size to, or smaller than the molecules forming the OA matrix (Evoy, 2020):

$$D_{H2O}(T, RH) = D^{\circ}{}_{H2O}(T) \times \left(\frac{\eta^{\circ}{}_{H2O}(T)}{\eta(T,\ RH)}\right)^{\xi} \quad \text{(S4)}$$

In this equation, $D^{\circ}{}_{H_2O}(T)$ is the self-diffusion of water calculated with the Stokes-Einstein equation at 290 K (2.12×10^{-9} m^2 s^{-1}). $\eta^{\circ}{}_{H2O}(T)$ is the viscosity of pure water obtained from literature with a value of ~1×10^{-3} Pa·s at 290 K (Weight, 2019). $\eta(T, RH)$ is the measured viscosity of the $PM_{2.5}$ droplet at the corresponding RH and temperature. ξ is the fractional exponent obtained using Eq. (S5), which accounts for the relative size of the diffusing molecule and the surrounding OA matrix:

$$\xi = 1 - \left[A \times exp\left(-B\frac{r_{diff}}{r_{matrix}}\right)\right] \quad \text{(S5)}$$

where coefficient values of A = 0.73 and B = 1.79 (Evoy et al., 2020), the hydrodynamic radius of water was taken as r_{diff} = 0.1 nm (Price et al., 2016), and the hydrodynamic radius of the matrix molecule was fixed at $r_{\text{matrix}} = 0.44$ nm, adopted from Evoy et al. (2020) where it was derived from molecular-weight and liquid-density data for sucrose, consistent with prior aerosol viscosity studies employing the fractional Stokes–Einstein framework (Maclean et al., 2021; Kiland et al., 2023). Using this value in Eq. (S5) yields a fractional exponent of ξ = 0.51. The conditioning time used in this study is summarized in Table S1.

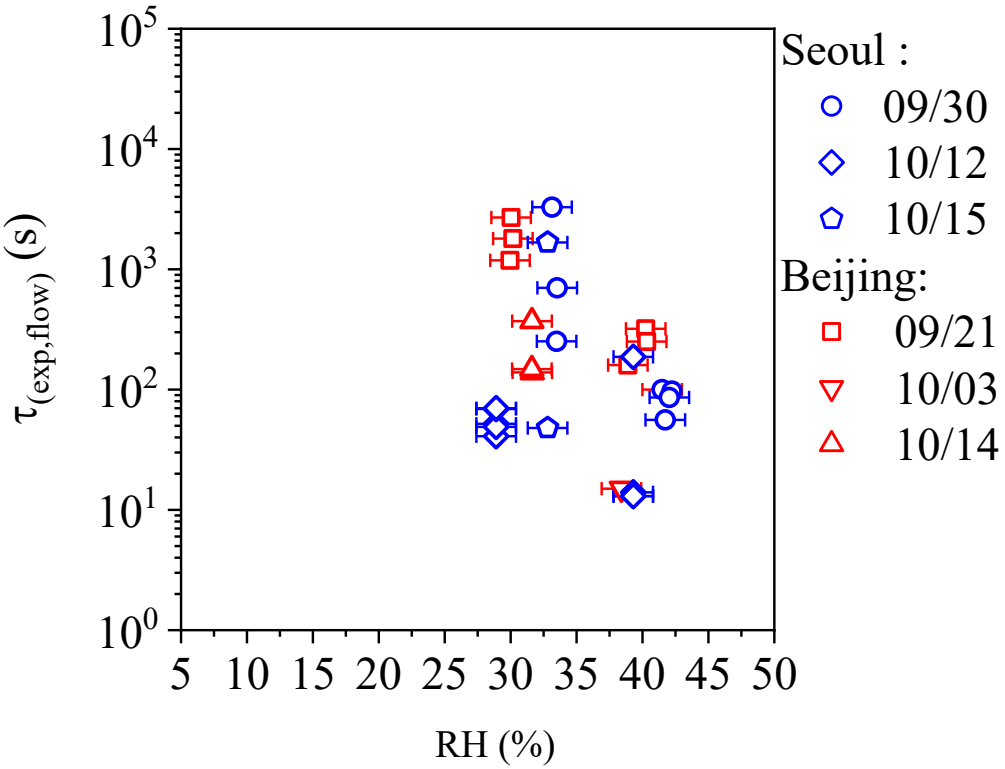

Figure S1. Characteristic experimental flow time $\tau_{(exp,\ flow)}$ of $PM_{2.5}$ droplets determined using the poke-and-flow technique for samples collected on different dates in Seoul and Beijing. Each symbol represents an individual $\tau_{(exp,\ flow)}$ value obtained by poking a single particle at a specific RH. The *x*-axis error bars represent the RH sensor uncertainty (±1.5 %), as determined from our RH sensor calibration in the flow cell.

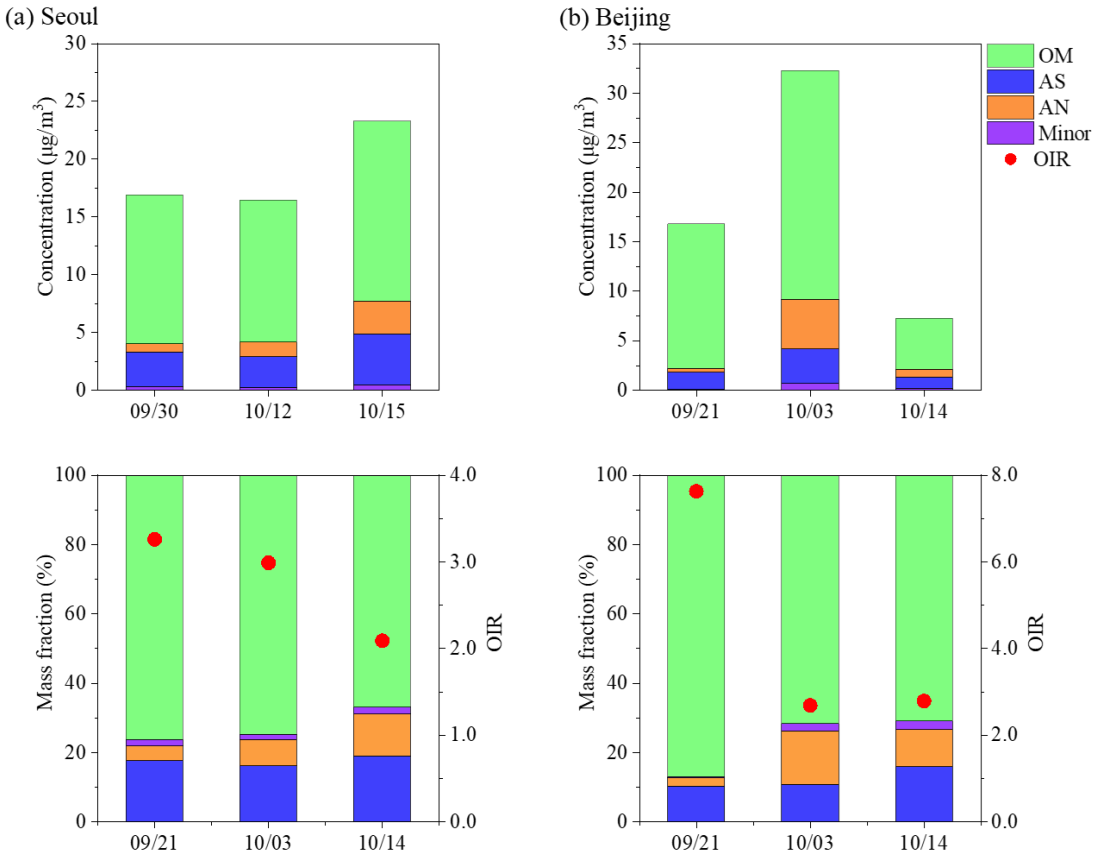

Figure S2. Chemical composition of $PM_{2.5}$ in (a) Seoul and (b) Beijing. For each site, the upper panel shows the concentrations of total $PM_{2.5}$ and its major components, including organic matter (OM), ammonium sulphate (AS), ammonium nitrate (AN), and minor inorganic ions such as Cl^-, Na^+, Ca^{2+}, K^+, and Mg^{2+}. The lower panel shows the corresponding mass fractions (%). The mean OM concentration was estimated by subtracting the measured inorganic components from the total $PM_{2.5}$ concentration.

Table S1. Overview of conditioning times for $PM_{2.5}$ droplets under different RH conditions. The parameter τ_{mix,H_2O} represents the characteristic timescale for internal water mixing time within the droplets, derived from the water diffusion coefficient inferred from viscosity at the corresponding RH. The term $\tau_{conditioning}$ refers to the experimentally defined period during which droplets were held at a specified RH to equilibrate with the surrounding gas phase. Calculations were based on a 40 μm droplet diameter, representing the upper-limit droplet size used in the poke-and-flow experiments.

Sample	**RH**	$\tau_{conditioning}$ **(h)**	τ_{mix,H_2O} **(h)**	$\tau_{conditioning} / \tau_{mix,H_2O}$
Seoul (09/30)	41	1.0	0.13	7.6
Seoul (09/30)	33	1.0	0.54	1.9
Seoul (10/12)	39	1.0	0.21	4.7
Seoul (10/12)	29	1.0	0.10	10.5
Seoul (10/12)	33	1.0	0.46	2.2
Beijing (09/21)	40	1.0	0.25	3.9
Beijing (09/21)	30	1.0	0.99	1.0
Beijing (10/03)	38	1.0	0.04	23.0
Beijing (10/14)	32	1.0	0.22	4.6

References

An, Y., Xu, J., Feng, L., Zhang, X., Liu, Y., Kang, S., Jiang, B., and Liao, Y.: Molecular characterization of organic aerosol in the Himalayas: insight from ultra-high-resolution mass spectrometry, Atmos. Chem. Phys., 19, 1115–1128, https://doi.org/10.5194/acp-19-1115-2019, 2019.

Choi, J. H., Ryu, J., Jeon, S., Seo, J., Yang, Y.-H., Pack, S. P., Choung, S., and Jang, K.-S.: In-depth compositional analysis of water-soluble and -insoluble organic substances in fine (PM2.5) airborne particles using ultra-high-resolution 15T FT-ICR MS and GC×GC-TOFMS, Environ. Pollut., 225, 329–337, https://doi.org/10.1016/j.envpol.2017.02.058, 2017.

Evoy, E.: The relationship between diffusion coefficients and viscosity in organic-water matrices as proxies for secondary organic aerosol, PHD thesis, The University of British Columbia, Vancouver, Canada, 2020.

Evoy, E., Kamal, S., Patey, G. N., Martin, S. T., and Bertram, A. K.: Unified description of diffusion coefficients from small to large molecules in organic–water mixtures, J. Phys. Chem. A, 124, 2301–2308, https://doi.org/10.1021/acs.jpca.9b11271, 2020.

Evoy, E., Kiland, K. J., Huang, Y., Schnitzler, E. G., Maclean, A. M., Kamal, S., Abbatt, J. P. D., and Bertram, A. K.: Diffusion coefficients and mixing times of organic molecules in β-caryophyllene secondary organic aerosol (SOA) and biomass burning organic aerosol (BBOA), ACS Earth Space Chem., 5, 3268–3278, https://doi.org/10.1021/acsearthspacechem.1c00317, 2021.

Kiland, K. J., Mahrt, F., Peng, L., Nikkho, S., Zaks, J., Crescenzo, G. V., and Bertram, A. K.: Viscosity, glass formation, and mixing times within secondary organic aerosol from biomass burning phenolics, ACS Earth Space Chem., 7, 1388–1400, https://doi.org/10.1021/acsearthspacechem.3c00039, 2023.

Kim, J. Y., Kim, Y. P., Yu, X., Yu, J., Wu, Z., Lee, H.-M., Song, M., Jang, K. S., Kim, C., Choi, N. R., and Lee, J. Y.: Concentrations and formation pathways of nitrogen-containing organic compounds in PM2.5 from Seoul and Beijing, Environ. Res. , 286, 122959, https://doi.org/10.1016/j.envres.2025.122959, 2025.

Kim, N. K., Kim, Y. P., Ghim, Y. S., Song, M. J., Kim, C. H., Jang, K. S., Lee, K. Y., Shin, H. J., Jung, J. S., Wu, Z., Matsuki, A., Tang, N., Sadanaga, Y., Kato, S., Natsagdorj, A., Tseren-Ochir, S., Baldorj, B., Song, C.-K., and Lee, J. Y.: Spatial distribution of PM2.5 chemical components during winter at five sites in Northeast Asia: High temporal resolution measurement study, Atmos. Environ., 290, 119359, https://doi.org/10.1016/j.atmosenv.2022.119359, 2022.

Lan, Z., Zhang, B., Huang, X., Zhu, Q., Yuan, J., Zeng, L., Hu, M., and He, L.: Source apportionment of PM2.5 light extinction in an urban atmosphere in China, J. Environ. Sci., 63, 277–284, https://doi.org/10.1016/j.jes.2017.07.016, 2018.

Maclean, A. M., Li, Y., Crescenzo, G. V., Smith, N. R., Karydis, V. A., Tsimpidi, A. P., Butenhoff, C. L., Faiola, C. L., Lelieveld, J., Nizkorodov, S. A., Shiraiwa, M., and Bertram, A. K.: Global Distribution of the Phase State and Mixing Times within Secondary Organic Aerosol Particles in the Troposphere Based on Room-Temperature Viscosity Measurements, ACS Earth Space Chem., 5, 3458–3473, https://doi.org/10.1021/acsearthspacechem.1c00296, 2021.

Price, H. C., Mattsson, J., and Murray, B. J.: Sucrose diffusion in aqueous solution, Phys. Chem. Chem. Phys., 18, 19207–19216, https://doi.org/10.1039/c6cp03238a, 2016.

Qiu, Y., Wu, Z., Man, R., Zong, T., Liu, Y., Meng, X., Chen, J., Chen, S., Yang, S., and Yuan, B.: Secondary aerosol formation drives atmospheric particulate matter pollution over megacities (Beijing and Seoul) in East Asia, Atmos. Environ., 301, 119702, https://doi.org/10.1016/j.atmosenv.2023.119702, 2023.

Smith, N. R., Crescenzo, G. V., Huang, Y. Z., Hettiyadura, A. P. S., Siemens, K., Li, Y., Faiola, C. L., Laskin, A., Shiraiwa, M., Bertram, A. K., and Nizkorodov, S. A.: Viscosity and liquid-liquid phase separation in healthy and stressed plant SOA, Environ. Sci.: Atmos., 1, 140–153, https://doi.org/10.1039/d0ea00020e, 2021.

Song, M., Jeong, R., Kim, D., Qiu, Y., Meng, X., Wu, Z., and Ahn, J.: Comparison of phase states of PM2.5 over megacities, Seoul and Beijing, and their implications on particle size distribution, Environ. Sci. Technol., 56, 17581–17590, https://doi.org/10.1021/acs.est.2c06377, 2022.

Song, M., Li, Y., Seong, C., Yang, H., Jang, K.-S., Wu, Z., Lee, J. Y., Matsuki, A., and Ahn, J.: Direct observation of liquid–liquid phase separation and core–shell morphology of PM2.5 collected from three Northeast Asian cities and implications for N2O5 hydrolysis, ACS ES&T Air, 2, 1079–1088, https://doi.org/10.1021/acsestair.5c00043, 2025.

Weight, W. D.: Practical Hydrogeology: Principles and field applications, McGraw Hill Professional, Newyork, 2019.

Won, S. R., Lee, K., Song, M., Kim, C., Jang, K.-S., and Lee, J. Y.: Characteristic of PM2.5 concentration and source apportionment during winter in Seosan, Korea, Asian J. Atmos. Environ., 18, 22, https://doi.org/10.1007/s44273-024-00044-x, 2024.

Xue, Q., Liu, X., Tian, Y., and Feng, Y.: Variations of inhalation risks during different heavy pollution episodes based on 3-year measurement of toxic components in size-segregated particles, Sci. Total Environ., 880, 163234, https://doi.org/10.1016/j.scitotenv.2023.163234, 2023.